RNA-Sequencing of Long-Term Label-Retaining Colon Cancer Stem Cells Identifies Novel Regulators of Quiescence

Joseph L. Regan[1,2,12*], Dirk Schumacher[3,4], Stephanie Staudte[1,2], Andreas Steffen[1], Ralf Lesche[1,5], Joern Toedling[1,5], Thibaud Jourdan[1], Johannes Haybaeck[6,7], Dominik Mumberg[1], David Henderson[1], Balázs Győrffy[8,9], Christian R.A. Regenbrecht[3,10,11], Ulrich Keilholz[2], Reinhold Schäfer[2,3,4], Martin Lange[1,5]

Affiliations

[1]Bayer AG, Drug Discovery, Pharmaceuticals, 13342 Berlin, Germany

[2]Charité Comprehensive Cancer Center, Charité - Universitätsmedizin Berlin, 10117 Berlin, Germany

[3]Laboratory of Molecular Tumor Pathology, Charité Universitätsmedizin Berlin, 10117 Berlin, Germany

[4]German Cancer Consortium (DKTK), DKFZ, 69120 Heidelberg, Germany

[5]Nuvisan ICB GmbH, 13343 Berlin, Germany

[6]Department of Pathology, Neuropathology and Molecular Pathology, Medical University of Innsbruck, Austria

[7]Diagnostic & Research Center for Molecular Biomedicine, Institute of Pathology, Medical University of Graz, Austria

[8]Department of Bioinformatics, Semmelweis University, 1094 Budapest, Hungary

[9]TTK Cancer Biomarker Research Group, Institute of Enzymology, 1117 Budapest, Hungary

[10]CELLphenomics GmbH, 13125 Berlin, Germany

[11]Institute of Pathology, University Medical Center Göttingen, 37075 Göttingen, Germany

[12]Lead Contact

*Correspondence: joseph.regan@charite.de (J.L.R.)

SUMMARY

Recent data suggests that colon tumors contain a subpopulation of therapy resistant quiescent cancer stem cells (qCSCs) that are the source of relapse following treatment. Here, using colon cancer patient-derived organoids (PDOs) and xenograft (PDX) models, we identify a rare population of long-term label-retaining ($PKH26^{Positive}$) qCSCs that can re-enter the cell cycle to generate new tumors. RNA-sequencing analyses demonstrated that these cells are enriched for stem cell associated gene sets such as Wnt and hedgehog signaling, epithelial-to-mesenchymal transition (EMT), embryonic development, tissue development and p53 pathway but have downregulated expression of genes associated with cell cycle, transcription, biosynthesis and metabolism. Furthermore, qCSCs are enriched for p53 interacting negative regulators of cell cycle, including *AKAP12, CD82, CDKN1A, FHL2, GPX3, KIAA0247, LCN2, TFF2, UNC5B* and *ZMAT3*, that we show are indicators of poor prognosis and may be targeted for qCSC abolition. Interestingly, CD82, KIAA0247 and UNC5B proteins localize to the cell surface and may therefore be potential markers for the prospective isolation of qCSCs. These data support the temporal inhibition of p53 signaling for the elimination of qCSCs and prevention of relapse in colorectal cancer.

INTRODUCTION

Molecular and functional intra-tumoral heterogeneity contribute to differences in treatment outcomes between colorectal cancer (CRC) patients with similar mutational profiles[1]. Studies of functional heterogeneity, as defined by phenotypic differences between cells, suggest that cancer stem cells (CSCs) are responsible for tumor growth, metastasis and therapy resistance[2–7]. CSCs share many of the characteristics of normal tissue stem cells, including unlimited self-renewal, the ability to generate differentiated daughter cells and chemoresistance[8,9].

The normal intestine is maintained by highly clonogenic crypt base LGR5^{Positive} stem cells and also contains a population of rare quiescent (G0 phase) stem cells that act as a clonogenic reserve capable of re-entering the cell cycle upon perturbation of tissue homeostasis, e.g. after injury leading to loss of the cycling crypt base stem cells[10–15]. Cancer often recapitulates the cellular hierarchy of the tissue in which it arises, and recent evidence suggests that many tumor types contain rare slow cycling / qCSCs[16–27]. Conventional chemotherapies and radiotherapies target proliferating cells and require active cycling for induction of apoptosis[1]. In addition, cellular quiescence has been shown to facilitate immune evasion[28]. Thus, non-dividing qCSCs may escape conventional therapeutic strategies and represent the source of disease relapse after treatment[2,29–31].

Cell cycle activation in qCSCs has been proposed as a therapeutic strategy to sensitize qCSCs to treatment and lead to long-term disease-free survival without relapse[29,30].

However, the molecular profiling of qCSCs for the identification of novel cell cycle regulators that do not also perturb cellular homeostasis in healthy tissues has been limited by both the rarity of qCSCs and the small number of suitable experimental assays available for their detection. PDOs echo the morphological, differentiation, intratumor mutational and drug sensitivity status of the original tumor[32,33] and thus provide an excellent model for the prospective isolation and profiling of qCSCs.

Strategies for the identification of quiescent cells employ pulse-chase approaches, including label retention (e.g. BrdU, PKH26, CFSE), wherein dividing cells lose the label and quiescent or slow cycling cells retain the label for an extended period of time, or the dilution of histone 2B-GFP (H2B-GFP)[34]. In contrast to the H2B-GFP approach[35], which can identify transient quiescent cells, label retention allows for the identification of cells that remain quiescent from the early stages of tumorigenesis. This is important since cells selectively surviving chemotherapy have been shown to be the same cells that are quiescent/slow cycling in untreated tumors and not cells that became quiescent upon drug treatment[36]. Such label-retaining cells (LRCs) have previously been reported in colon cancer cell lines, xenografts and, more recently, in PDOs[6,36–38].

However, to date, the transcriptomic profiling of qCSCs in CRC patients has been limited to microarray analyses of transiently slow-cycling H2B-GFP^{Positive} cells from a single CRC patient by Puig *et al*. (2018)[35] and of PKH26^{Positive} LRCs from two colon cancer patient-derived (via spheroid culture) xenograft models by Francescangeli *et al*. (2020)[36]. In addition, the LRCs reported in the latter study were not functionally tested for proliferative

or self-renewal capacity prior to molecular profiling and instead relied on expression of CD133 as evidence of a stem cell phenotype. CD133 expression is not restricted to stem cells of the intestine and is expressed on both CSC and differentiated tumor cells[39–42].

Here, we report the identification and first whole-transcriptome RNA-sequencing analyses of label-retaining qCSCs in a panel of PDOs encompassing primary colon tumors and metastases. These cells maintain a large proliferative capacity, persist long term *in vivo* and display the molecular hallmarks of quiescent tissue stem cells[43], including enrichment for p53 pathway and developmental gene sets alongside downregulation of cell cycle, transcription, biosynthesis and metabolism genes. In addition, we show that qCSCs are enriched for p53 interacting negative regulators of cell cycle that we propose may be targeted for cell cycle activation and the elimination of qCSCs. These data provide a valuable resource for the development of novel therapeutic strategies geared toward the elimination of minimal residual disease and the prevention of relapse.

RESULTS

Colon cancer PDOs contain rare label-retaining qCSCs that persist long term *in vivo*

To determine whether PDOs contain non-cycling LRCs, we performed an initial 72 h pulse chase experiment using CM-DiL dye. PDOs were established as previously described[44,45], processed to single cells, uniformly labelled with CM-DiL dye and seeded in Matrigel culture. CM-DiL is diluted with each cell division, halving its fluorescence

between each daughter cell until it becomes undetectable. Non-cycling cells can thus be identified by their label retention. After 72 h the majority of PDO cells had lost the CM-DiL dye but some PDOs contained non-cycling LRCs (Figure 1A). To determine the frequency of these non-cycling (G0) cells we performed EdU cell cycle analysis on a panel of colon cancer PDOs (Table S1). This analysis demonstrated that PDOs contain non-cycling cells that do not proliferate and remain in G0 within a 72 h period (Figure 1B and C).

To determine the long-term proliferative capacity of these non-cycling cells, we labelled cells with the lipophilic fluorescent dye PKH26. Unlike CM-DiL, which is suitable for short term label retention studies, PKH26 labelling can be used to identify non-cycling cells for up to six months (*in vitro* and *in vivo*)[46,47]. PDOs were dissociated to single cells, labelled with PKH26 and replated in Matrigel culture. After 12 days PDOs were re-processed to single cells and analyzed by fluorescence assisted cell sorting (FACS). These data demonstrated that PDOs contain rare, non-cycling, long-term LRCs (Figure 2A and B). Crucially, FACS isolation and replating of $PKH26^{Positive}$ $DAPI^{Negative}$ (live) cells from 12 day cultures demonstrated that they are not label-retaining due to terminal differentiation or senescence but can re-enter the cell cycle to generate organoids and have a large proliferative capacity (Figure 2C – F). In addition, non-adherent spheroid formation assays, the gold standard assay for testing stem cell function *in vitro*[48,49], showed that $PKH26^{Positive}$ cells are enriched for self-renewing CSCs (Figure 2G).

In order to test whether these cells also persisted long-term *in vivo* we generated xenografts by transplanting PKH26 labelled cells. Long-term tracking of LRCs in

xenografts requires the slow growth of the tumor. Cells were therefore transplanted at a low cell number based on knowledge of tumor growth rates from previous limiting dilution xenotransplantation assays, in which xenografts were generated from 1,000 PDO cells[44].

Unlabeled cells, lacking the burden of carrying a fluorescent dye may be at a competitive advantage over labelled cells. Therefore, immediately prior to transplantation, PKH26 labelled cells were processed by FACS to exclude unlabelled cells and thus ensure that only live ($DAPI^{Negative}$) PKH26 labelled cells would give rise to tumors. Significantly, analysis of xenograft tissue demonstrated the presence of $PKH26^{Positive}$ LRCs for up to 80 days after transplantation (Figure 2H). Previous studies have observed quiescence to be a transient state[35]. However, these data demonstrate that quiescence can be stable and persist long-term from the initial stages of tumor development.

RNA-sequencing of $PKH26^{Positive}$ cells reveals a molecular signature of qCSCs

To generate a molecular profile of qCSCs we carried out RNA-sequencing analyses of $PKH26^{Negative}$ (cycling) and $PKH26^{Positive}$ (non-cycling) qCSCs isolated from a panel of six different PDO models (Table S1) after 12 days in Matrigel culture. These data demonstrated that $PKH26^{Positive}$ qCSCs are enriched for stem cell associated gene sets, such as embryonic development, organ development, placenta, nervous system development, EMT, Wnt and hedgehog signaling (Figure 3A).

At the same time as showing enrichment for genes associated with growth and development, $PKH26^{Positive}$ qCSCs have downregulated cell cycle, transcription, protein

synthesis, metabolism and biosynthesis genes (Figure 3B and C). These data are in agreement with the transcriptional profiles of slow cycling / qCSCs reported in previous studies[35–37] and demonstrate a common molecular signature of qCSCs.

The normal intestine also contains quiescent stem cells that can regenerate the damaged intestine upon loss of crypt base stem cells following injury, although whether cellular plasticity or distinct cell types are responsible for this remains unclear. Bmi1[50], Hopx[51], Lrig1[52] and Tert[53] have previously been reported as markers of quiescent "+4" stem cells, although subsequent studies have shown that actively cycling crypt base stem cells also express these markers at equivalent levels[54]. Similarly, we did not detect enhanced expression of these markers in qCSCs. This is also in agreement with a recent single-cell RNA-sequencing analyses of the regenerating mouse intestine that identified a damage-induced quiescent cell type termed revival stem cells (revSCs)[15]. These cells, required for the regeneration of a functional intestine, are extremely rare during normal homeostasis and are characterised by enhanced expression of the pro-survival stress response gene Clu[55]. Interestingly, we find that many of the genes that make up the molecular signature of these quiescent revSCs are also enriched in qCSCs and have been found to regulate therapy resistance in various types of cancer. These common genes include *CLU*[56], *CTSD*[57,58], *CDKN1A*[59–63], *EMP1*[64,65], *MUC3*[66], *LAMC2*[67], *KRT19*[68], *LGALS3*[69], *F3*, *ITM2B*, *ITGB4*[70,71], *CDH17*[72,73] and *GSN*[74,75] (Figure 3E – F, Figure S1 and Supplementary Data File 1). Considering that colon cancer is a heterogeneous tumor that recapitulates the cellular hierarchy of the intestine, these data suggest that the qCSCs identified here may be the tumor equivalent of revSCs. However, in contrast to

185 revSCs and previous studies on qCSCs, our data demonstrate that qCSCs are enriched
186 for p53 signaling (Figure 3A).
187
188 **qCSCs are dependent on p53 signaling**
189 Loss of p53 in hematopoietic (HSCs) and neural stem cells (NSCs) causes these cells to
190 exit quiescence and enter the cell cycle[76–78]. Targeting p53 may have the same effect in
191 qCSCs but is complicated by the role of p53 as a tumor suppressor and guardian of
192 homeostasis[79]. However, targeting negative cell cycle regulators downstream of p53 may
193 provide novel strategies for qCSC elimination without affecting the role of p53 in healthy
194 cells. Differential gene expression analysis, comparing PKH26^{Negative} and PKH26^{Positive}
195 cells, identified the negative cell-cycle regulators *AKAP12*[80–83], *CD82*[84], *CDKN1A*[85–88],
196 *FHL2*[89–92], *GPX3*[93–95], *KIAA0247*[96,97], *LCN2*[98–100], *TFF2*[101–105], *UNC5B*[106–108] and
197 *ZMAT3*[109,110] to be enriched in qCSCs (Figure 3D). Significantly, each of these genes is
198 a target of p53[79,80,82,92,96,109,111–115], and with the exceptions of LCN2 and *ZMAT*3,
199 associated with reduced survival in CRC (Figure 4A). Interestingly, CD82, KIAA0247 and
200 UNC5B proteins localize to the cell surface and may therefore have potential as new
201 markers for the prospective isolation of qCSCs in CRC. Indeed, CD82 has previously
202 been identified as a marker for prospectively isolating stem cells from human fetal and
203 adult skeletal muscle and is a functional surface marker of long-term HSCs[84,116].
204
205 Deletion of *CDKN1A* (P21), which is the downstream mediator of p53 induced cell cycle
206 arrest[86,117], leads to cell cycle activation and exhaustion of quiescent HSCs and
207 NSCs[118,119]. In addition, *CDKN1A* is highly expressed in noncycling intestinal crypt base

stem cells[52] and revSCs[15]. We therefore selected *CDKN1A* as a candidate gene to determine whether targeting the p53 pathway would eliminate qCSCs. Significantly, shRNA mediated knockdown of *CDKN1A* (Figure S3) in PKH26 labelled qCSCs resulted in the elimination of PKH26^{Positive} label-retaining qCSCs (Figure 4B and C).

DISCUSSION

Colon cancer is a heterogeneous tumor entity containing a subpopulation of qCSCs that may promote tumor cell heterogeneity, plasticity, and resistance to various types of stress, including resistance to conventional treatments[29]. However, the rarity and plasticity of qCSCs has made them an elusive and challenging cell state to define and target. Here, we provide the first whole-transcriptome analyses of a population of colon cancer patient-derived long-term label-retaining qCSCs and identify genes that may provide novel targets for their elimination.

Label retention has previously been used as a strategy for the isolation of both healthy quiescent tissue stem cells and qCSCs from a variety of cancer types[11,17,25,26,29,120–122]. In agreement with these studies, we show that PKH26^{Positive} LRCs isolated from colon cancer PDOs are qCSCs capable of entering the cell cycle and self-renewing after replating in adherent and non-adherent cell culture conditions and maintain long-term quiescence in xenograft models. Interestingly, *in vivo* these cells were located at the tumor border, suggesting that quiescence may be induced at the invasive tumor front where such cells may be primed for metastatic dissemination. This is in agreement with

previous studies showing cell cycle arrest / decreased proliferation and increased levels of Wnt signaling at the invasive front of colorectal tumors[123–127].

RNA-sequencing of qCSCs demonstrated that they display the molecular hallmarks of quiescence[128] while also being enriched for the same developmental and stem cell associated gene sets previously described for actively cycling ALDH^{Positive} CSCs[44], which unlike PKH26^{Positive} LRCs are enriched in PDOs.

We previously reported that hedgehog signaling in active colon CSCs is non-canonical (SHH-dependent, PTCH-dependent, SMO-independent, GLI-independent) and acts as a positive regulator of Wnt signaling for CSC survival[44]. In agreement with our work, a subsequent study from Buczacki *et al*. (2018) demonstrated that qCSC survival in CRC is also dependent on non-canonical hedgehog signaling mediated regulation of Wnt signaling[37]. In addition, several of the genes common to both the revSCs reported by Ayyaz *et al* (2019)[15] and qCSCs, namely CLU[129], CTSD[130], CDKN1A[131], EMP1[132], MUC3[133], LAMC2[134], KRT19[135], LGALS3[136], *F3*[137,138], ITGB4[139], CDH17[140] and GSN[141], are targets and/or regulators of Wnt signaling. Overall, these data demonstrate that both cycling and non-cycling CSCs share overlapping molecular profiles and further support the targeting of non-canonical hedgehog signaling to prevent disease relapse[37,44,142].

However, the molecular mechanisms that distinguish non-cycling qCSCs from cycling CSCs required further elucidation. p53 plays a crucial role in regulating cellular stress responses such as DNA-damage repair, senescence, apoptosis and cell cycle arrest in

253 virtually all cell types[87,143]. In addition, it is an important regulator of stem cell self-renewal
254 and differentiation in embryonic and adult tissue stem cells[77,144,145] and cancer stem
255 cells[146–148]. Significantly, it has also been demonstrated to be essential for the
256 maintenance of quiescence in HSCs, NSCs, muscle stem cells and lung progenitor
257 cells[76,78,149–151].
258
259 Here we show that qCSCs, in contrast to cycling ALDH^{Positive} CSCs[44], are enriched for
260 p53 signaling genes. p53 is mutated in 40 - 50% of CRCs. Reflecting this, half the tumors
261 included in our study contain a p53 mutation (Table S1). However, regardless of mutation
262 status, p53 appears to be functional in all the PDO models analyzed, as observed by p53-
263 dependent expression of *CDKN1A* (Figure 3D)[152,153].
264
265 Inhibiting the p53 pathway may therefore provide novel therapeutic “lock-out” strategies
266 to induce the proliferation of qCSCs and thereby sensitize them to chemotherapeutics
267 and prevent relapse[128,154,155]. Considering the role of p53 as a tumor suppressor and
268 guardian of homeostasis in healthy tissues, as well as its inactivation in many cancers,
269 most strategies to date have focused on the development of p53 activators[156]. However,
270 our data, and others, suggest that strategies that activate p53 may lead to therapy
271 resistance. For example, in breast cancer p53 induces senescence, drives resistance to
272 therapy and is associated with poor therapeutic response and overall survival[157,158].
273
274 Inhibiting p53 could interfere with its role in normal tissue homeostasis or lead to the
275 activation of senescent cancer cells in other tissues. However, healthy cells have lower

p53 expression levels than cancer cells[159] and single dose treatments, that avoid the unwanted consequences of sustained p53 inhibition, may be sufficient to eliminate qCSCs. This was recently demonstrated by Webster *et al.* (2020) in melanoma, where a single dose of p53 inhibitor during the early stage of BRAF/MEK inhibitor treatment resulted in improved response to therapy[160].

In addition, targeting negative cell cycle regulators downstream of p53, such as those identified here (*AKAP12*[80–83], *CD82*[84,112], *CDKN1A*[85–88], *FHL2*[89–92], *GPX3*[93–95], *KIAA0247*[96,97], *LCN2*[98–100,115], *TFF2*[101–105], *UNC5B*[106–108] and *ZMAT3*[109,110]), may provide novel strategies for activating cell cycle in qCSCs without affecting the role of p53 in healthy cells. For example, p53-dependent activation of p21 (*CDKN1A*), which we show is required for the maintenance of qCSCs, is an important axis in senescence-dependent tumor suppression. However, despite p21 playing an important role in mediating the p53-dependent cellular response to stress, lack of p21 does not promote tumor development[161]. Furthermore, p21 maintains CSC self-renewal, limits proliferation and confers therapy resistance in numerous cancers types in which its temporal inhibition has been proposed as a strategy to overcome resistance to DNA-damaging chemotherapy and radiation[60–63,162–166]. Indeed, several small molecule inhibitors of p21 have been reported, including butyrolactone I[167], LLW10[168], sorafenib[169] and UC2288[170], that could serve as novel drugs for the elimination of therapy resistant qCSCs.

These data demonstrate the existence of long-term p53-dependent qCSCs in colon cancer and provide evidence supporting the temporal inhibition of p53 signaling, in

299 combination with standard-of-care treatments, for the elimination of qCSCs and
300 prevention of disease relapse. The p53 target genes identified here, along with the
301 publication of our qCSC whole-transcriptome data, will provide a valuable resource for
302 the development of such therapeutic strategies in the future.
303
304 **EXPERIMENTAL PROCEDURES**
305
306 **Human tissue samples and establishment of patient-derived cancer organoid cell**
307 **cultures**
308 Tumor material was obtained with informed consent from CRC patients under approval
309 from the local Institutional Review Board of Charité University Medicine (Charité Ethics
310 Cie: Charitéplatz 1, 10117 Berlin, Germany) (EA 1/069/11) and the ethics committee of
311 the Medical University of Graz and the ethics committee of the St John of God Hospital
312 Graz (23-015 ex 10/11). Tumor staging was carried out by experienced and board-
313 certified pathologists (Table S1). Cancer organoid cultures were established and
314 propagated as described[45,171].
315
316 **Cell cycle analysis and colony forming assays**
317 Cell cycle analysis was carried using the Click-iT EdU assay (Invitrogen, #C10337) and
318 assessed by FACS on a BD LSR II analyzer. For colony forming assays, PDOs were
319 processed to single cells and labelled with CellTracker™ CM-DiI fluorescent dye (C7000,
320 Thermo Fisher) or PKH26 (PKH26GL, Sigma-Aldrich) following manufacturer's
321 instructions and DAPI (to exclude dead cells). $PKH26^{Positive}$ $DAPI^{Negative}$ (live) cells were

sorted by FACS (BD FACS Aria II) into adherent Matrigel culture. After 12 days, PDOs were once again processed to single cells and sorted by FACS, seeding $PKH26^{Positive}$ $DAPI^{Negative}$ cells and $PKH26^{Negative}$ $DAPI^{Negative}$ cells separately at limiting dilution into 96-well adherent Matrigel and 384-well non-adherent ultra-low attachment plates at a frequency of 100 and 1 cell per well, respectively. The purity of the sorted $PKH26^{Positive}$ cell population was confirmed by post-sort FACS analysis. PDO sizes were determined by ImageJ software analysis. Ultra-low attachment wells containing spheroids were counted and used to calculate the CSC frequency using ELDA software (http://bioinf.wehi.edu.au/software/elda/index.html; Hu and Smyth, 2009).

Xenotransplantation

Housing and handling of animals followed European and German Guidelines for Laboratory Animal Welfare. Animal experiments were conducted in accordance with animal welfare law, approved by local authorities, and in accordance with the ethical guidelines of Bayer AG. PDOs were processed to single cells and labelled with PKH26 (PKH26GL, Sigma-Aldrich) following manufacturer's instructions and DAPI (to exclude dead cells). $PKH26^{Positive}$ $DAPI^{Negative}$ cells were collected by FACS and immediately transplanted by injected subcutaneously in PBS and Matrigel (1:1 ratio) into female 8 – 10-week-old $nude^{-/-}$ mice at 1000 cells per animal. The purity of the sorted $PKH26^{Positive}$ cell population was confirmed by post-sort FACS analysis.

Immunofluorescence staining

Tumors were fixed in 4% paraformaldehyde overnight and cryopreserved in OCT compound. Immunohistochemistry of frozen sections was carried out via standard techniques with α-Tubulin (T5168, mouse monoclonal, Sigma; diluted 1:1000) and a secondary conjugated antibody at room temperature for 2 hours. For immunofluorescence imaging of PDOs, cultures were fixed in 4% paraformaldehyde for 30 min at room temperature and permeabilized with 0.1% Triton X-100 for 30 min and blocked in phosphate-buffered saline (PBS) with 10% bovine serum albumin (BSA). F-actin was stained with Alexa Fluor® 647 Phalloidin (#A22287, Thermo Fisher; diluted 1:20) for 30 min at room temperature. Nuclei were counterstained with DAPI. Negative controls were performed using the same protocol with substitution of the primary antibody with IgG-matched controls. Cancer organoids were then transferred to microscope slides for examination using a Zeiss LSM 700 Laser Scanning Microscope.

RNA Sequencing

Cells were lysed in RLT buffer and processed for RNA using the RNeasy Mini Plus RNA extraction kit (Qiagen). Samples were processed using NuGEN's Ovation RNA-Seq System V2 and Ultralow V2 Library System and sequenced on an Illumina HiSeq 2500 machine as 2x125nt paired-end reads. The raw data in Fastq format were checked for sample quality using our internal NGS QC pipeline. Reads were mapped to the human reference genome (assembly hg19) using the STAR aligner (version 2.4.2a). Total read counts per gene were computed using the program "featureCounts" (version 1.4.6-p2) in the "subread" package, with the gene annotation taken from Gencode (version 19).

Variance-stabilising transformation from the Bioconductor package DESeq2[172] was used for normalisation and differential-expression analysis.

Viral transduction

Cells were seeded in 100 µl volumes of antibiotic free culture media at 1.0 x10^5 cells per well in ultra-low attachment 96-well plates. Control and shRNA lentiviruses were purchased from Sigma-Aldrich (Table S2). Viral particles were added at a multiplicity of infection of 1. Cells were transduced for up to 96 h or until GFP positive cells were observed before being embedded in Matrigel for the establishment of lentiviral transduced cancer organoid cultures. Puromycin (2 µg/ml) was used to keep the cells under selection.

Gene expression analysis

For quantitative real-time RT-PCR analysis RNA was isolated using the RNeasy Mini Plus RNA extraction kit (Qiagen). cDNA synthesis was carried out using a Sensiscript RT kit (Qiagen). RNA was transcribed into cDNA using an oligo dTn primer (Promega) per reaction. Gene expression analysis was performed using TaqMan® Gene Expression Assays (Applied Biosystems) (Table S3) on an ABI Prism 7900HT sequence detection system (Applied Biosystems). GAPDH was used as an endogenous control and results were calculated using the Δ-ΔCt method. Data were expressed as the mean fold gene expression difference in three independently isolated cell preparations over a comparator sample with 95% confidence intervals. Survival curves were generated using the Kaplan-Meier Plotter (www.kmplot.com/analysis)[173]. Gene ontology enrichment analysis was carried out using the Gene Ontology Resource (www.geneontology.org)[174,175].

389

390 **Statistical analysis**

391 GraphPad Prism 8.0 was used for data analysis and imaging. All data are presented as
392 the means ± SD, followed by determining significant differences using the two-tailed t test.
393 Significance of RT-PCR data was determined by inspection of error bars as described by
394 Cumming *et al*. (2007)[176]. Gene set enrichment analysis was carried out using pre-ranked
395 feature of the Broad Institute GSEA software version 2 using msigdb v5.1 gene sets[177,178].
396 The ranking list was derived from the fold changes calculated from the differential gene
397 expression calculation and nominal p-values. P-values <0.05 were considered as
398 statistically significant. The representation factor and the associated probability of finding
399 an overlap were calculated using http://nemates.org/MA/progs/representation.stats.html.
400 Survival curves were generated using the Kaplan-Meier Plotter
401 (www.kmplot.com/analysis)[173]. For the final list of significant genes, False Discovery Rate
402 (FDR) was computed using the Benjamini-Hochberg method[179].

403

404 **Acknowledgements**

405 We thank Dorothea Przybilla, and Cathrin Davies (Laboratory of Molecular Tumor
406 Pathology, Charité Universitätsmedizin Berlin, Germany) for technical and cell culture
407 assistance. The research leading to these results has received support from the
408 Innovative Medicines Initiative Joint Undertaking under Grant Agreement 115234
409 (OncoTrack), the resources of which are composed of financial contribution from the
410 European Union Seventh Framework Programme (FP7/2007-2013) and EFPIA

411 companies in kind contribution. A.S., T.J., D.M. and. D.H. are employees of Bayer AG.
412 R.L., J.T. and M.L. are employees of Nuvisan ICB GmbH. C.R.A.R.
413
414 **Authors Contribution**
415 Conceptualization, J.L.R.; Methodology, J.L.R.; Investigation, J.L.R., D.S., S.S., A.S.,
416 R.L., J.T., T.J., J.H., and M.L.; Writing, J.L.R.; Visualization, J.L.R; Data Curation, A.S.,
417 J.T.; Resources, J.H., U.K., C.R.A.R. and B.G.; Supervision, J.L.R., D.M., D.H., R.S., and
418 M.L.
419
420 **Accession Numbers**
421 Array data are available in the ArrayExpress database (www.ebi.ac.uk/arrayexpress)
422 under accession number E-MTAB-8924.
423
424 **References**
425 1. Kreso, A. *et al.* Variable Clonal Repopulation Dynamics Influence Chemotherapy
426 Response in Colorectal Cancer. *Science (80-.).* **339**, 543–548 (2013).
427 2. De Angelis, M. L., Francescangeli, F., La Torre, F. & Zeuner, A. Stem Cell
428 Plasticity and Dormancy in the Development of Cancer Therapy Resistance .
429 *Frontiers in Oncology* **9**, 626 (2019).
430 3. Barker, N. *et al.* Crypt stem cells as the cells-of-origin of intestinal cancer. *Nature*
431 **457**, 608 (2008).
432 4. Shackleton, M., Quintana, E., Fearon, E. R. & Morrison, S. J. Heterogeneity in
433 cancer: cancer stem cells versus clonal evolution. *Cell* **138**, 822–9 (2009).

5. O'Brien, C. A., Pollett, A., Gallinger, S. & Dick, J. E. A human colon cancer cell capable of initiating tumour growth in immunodeficient mice. *Nature* **445**, 106–110 (2007).

6. Moore, N., Houghton, J. & Lyle, S. Slow-Cycling Therapy-Resistant Cancer Cells. *Stem Cells Dev.* **21**, 1822–1830 (2011).

7. Brock, A. & Huang, S. Precision Oncology: Between Vaguely Right and Precisely Wrong. *Cancer Res.* **77**, 6473 LP – 6479 (2017).

8. Reya, T., Morrison, S. J., Clarke, M. F. & Weissman, I. L. Stem cells, cancer, and cancer stem cells. *Nature* **414**, 105–111 (2001).

9. Sell, S. Stem cell origin of cancer and differentiation therapy. **51**, 1–28 (2004).

10. Clevers, H. A unifying theory for the crypt. *Nature* **495**, 53–54 (2013).

11. Buczacki, S. J. A. *et al.* Intestinal label-retaining cells are secretory precursors expressing Lgr5. *Nature* **495**, 65–69 (2013).

12. Barker, N. *et al.* Identification of stem cells in small intestine and colon by marker gene Lgr5. *Nature* **449**, 1003–7 (2007).

13. Cheng, H. & Leblond, C. P. Origin, differentiation and renewal of the four main epithelial cell types in the mouse small intestine V. Unitarian theory of the origin of the four epithelial cell types. *Am. J. Anat.* **141**, 537–561 (1974).

14. POTTEN, C. S. Extreme sensitivity of some intestinal crypt cells to X and γ irradiation. *Nature* **269**, 518–521 (1977).

15. Ayyaz, A. *et al.* Single-cell transcriptomes of the regenerating intestine reveal a revival stem cell. *Nature* **569**, 121–125 (2019).

16. Chen, J. *et al.* A restricted cell population propagates glioblastoma growth after

chemotherapy. *Nature* **488**, 522–526 (2012).

17. Dembinski, J. L. & Krauss, S. Characterization and functional analysis of a slow cycling stem cell-like subpopulation in pancreas adenocarcinoma. *Clin. Exp. Metastasis* **26**, 611 (2009).

18. Vanner, R. J. *et al.* Quiescent Sox2^{+} Cells Drive Hierarchical Growth and Relapse in Sonic Hedgehog Subgroup Medulloblastoma. *Cancer Cell* **26**, 33–47 (2014).

19. Zeuner, A. *et al.* Elimination of quiescent/slow-proliferating cancer stem cells by Bcl-XL inhibition in non-small cell lung cancer. *Cell Death Differ.* **21**, 1877–1888 (2014).

20. Ebinger, S. *et al.* Characterization of Rare, Dormant, and Therapy-Resistant Cells in Acute Lymphoblastic Leukemia. *Cancer Cell* **30**, 849–862 (2016).

21. Gao, M.-Q., Choi, Y.-P., Kang, S., Youn, J. H. & Cho, N.-H. CD24+ cells from hierarchically organized ovarian cancer are enriched in cancer stem cells. *Oncogene* **29**, 2672–2680 (2010).

22. Kabraji, S. *et al.* AKT1low quiescent cancer cells persist after neoadjuvant chemotherapy in triple negative breast cancer. *Breast Cancer Res.* **19**, 88 (2017).

23. Lagadinou, E. D. *et al.* BCL-2 Inhibition Targets Oxidative Phosphorylation and Selectively Eradicates Quiescent Human Leukemia Stem Cells. *Cell Stem Cell* **12**, 329–341 (2013).

24. Lin, W. *et al.* Dormant Cancer Cells Contribute to Residual Disease in a Model of Reversible Pancreatic Cancer. *Cancer Res.* **73**, 1821 LP – 1830 (2013).

25. Pece, S. *et al.* Biological and molecular heterogeneity of breast cancers correlates with their cancer stem cell content. *Cell* **140**, 62–73 (2010).

480 26. Roesch, A. *et al.* A Temporarily Distinct Subpopulation of Slow-Cycling Melanoma
481 Cells Is Required for Continuous Tumor Growth. *Cell* **141**, 583–594 (2010).
482 27. Saito, Y. *et al.* Induction of cell cycle entry eliminates human leukemia stem cells
483 in a mouse model of AML. *Nat. Biotechnol.* **28**, 275–280 (2010).
484 28. Malladi, S. *et al.* Metastatic Latency and Immune Evasion through Autocrine
485 Inhibition of WNT. *Cell* **165**, 45–60 (2016).
486 29. Moore, N. & Lyle, S. Quiescent, slow-cycling stem cell populations in cancer: a
487 review of the evidence and discussion of significance. *J. Oncol.* **2011**, 396076
488 (2011).
489 30. Chen, W., Dong, J., Haiech, J., Kilhoffer, M.-C. & Zeniou, M. Cancer Stem Cell
490 Quiescence and Plasticity as Major Challenges in Cancer Therapy. *Stem Cells*
491 *Int.* **2016**, 1740936 (2016).
492 31. Shen, S., Vagner, S. & Robert, C. Persistent Cancer Cells: The Deadly Survivors.
493 *Cell* **183**, 860–874 (2020).
494 32. Roerink, S. F. *et al.* Intra-tumour diversification in colorectal cancer at the single-
495 cell level. *Nature* **556**, 457–462 (2018).
496 33. Fujii, M. & Sato, T. Somatic cell-derived organoids as prototypes of human
497 epithelial tissues and diseases. *Nat. Mater.* **20**, 156–169 (2021).
498 34. Blanpain, C. & Simons, B. D. Unravelling stem cell dynamics by lineage tracing.
499 *Nat. Rev. Mol. Cell Biol.* **14**, 489–502 (2013).
500 35. Puig, I. *et al.* TET2 controls chemoresistant slow-cycling cancer cell survival and
501 tumor recurrence. *J. Clin. Invest.* **128**, 3887–3905 (2018).
502 36. Francescangeli, F. *et al.* A pre-existing population of ZEB2+ quiescent cells with

503 stemness and mesenchymal features dictate chemoresistance in colorectal
504 cancer. *J. Exp. Clin. Cancer Res.* **39**, 2 (2020).
505 37. Buczacki, S. J. A. *et al.* Itraconazole targets cell cycle heterogeneity in colorectal
506 cancer. *J. Exp. Med.* **215**, 1891 LP – 1912 (2018).
507 38. Francescangeli, F. *et al.* Proliferation State and Polo-Like Kinase1 Dependence of
508 Tumorigenic Colon Cancer Cells. *Stem Cells* **30**, 1819–1830 (2012).
509 39. Shmelkov, S. V *et al.* CD133 expression is not restricted to stem cells, and both
510 CD133+ and CD133– metastatic colon cancer cells initiate tumors. *J. Clin. Invest.*
511 **118**, 2111–2120 (2008).
512 40. Kemper, K. *et al.* The AC133 Epitope, but not the CD133 Protein, Is Lost upon
513 Cancer Stem Cell Differentiation. *Cancer Res.* **70**, 719 LP – 729 (2010).
514 41. Snippert, H. J. *et al.* Prominin-1/CD133 Marks Stem Cells and Early Progenitors
515 in Mouse Small Intestine. *Gastroenterology* **136**, 2187-2194.e1 (2009).
516 42. Glumac, P. M. & LeBeau, A. M. The role of CD133 in cancer: a concise review.
517 *Clin. Transl. Med.* **7**, 18 (2018).
518 43. Cheung, T. H. & Rando, T. A. Molecular regulation of stem cell quiescence. *Nat.*
519 *Rev. Mol. Cell Biol.* **14**, 329–340 (2013).
520 44. Regan, J. L. *et al.* Non-Canonical Hedgehog Signaling Is a Positive Regulator of
521 the WNT Pathway and Is Required for the Survival of Colon Cancer Stem Cells.
522 *Cell Rep.* **21**, 2813–2828 (2017).
523 45. Schütte, M. *et al.* Molecular dissection of colorectal cancer in pre-clinical models
524 identifies biomarkers predicting sensitivity to EGFR inhibitors. *Nat. Commun.* **8**,
525 (2017).

526 46. Horan, P. K., Melnicoff, M. J., Jensen, B. D. & Slezak, S. E. Chapter 42
527 Fluorescent Cell Labeling for in Vivo and in Vitro Cell Tracking. in 469–490
528 (1990). doi:10.1016/S0091-679X(08)60547-6
529 47. Cicalese, A. *et al.* The Tumor Suppressor p53 Regulates Polarity of Self-
530 Renewing Divisions in Mammary Stem Cells. *Cell* **138**, 1083–1095 (2009).
531 48. Ricci-Vitiani, L. *et al.* Identification and expansion of human colon-cancer-initiating
532 cells. *Nature* **445**, 111–115 (2007).
533 49. Weiswald, L.-B., Bellet, D. & Dangles-Marie, V. Spherical Cancer Models in
534 Tumor Biology. *Neoplasia* **17**, 1–15 (2015).
535 50. Yan, K. S. *et al.* The intestinal stem cell markers Bmi1 and Lgr5 identify two
536 functionally distinct populations. *Proc. Natl. Acad. Sci.* **109**, 466 LP – 471 (2012).
537 51. Takeda, N. *et al.* Interconversion between intestinal stem cell populations in
538 distinct niches. *Science* **334**, 1420–1424 (2011).
539 52. Powell, A. E. *et al.* The Pan-ErbB Negative Regulator Lrig1 Is an Intestinal Stem
540 Cell Marker that Functions as a Tumor Suppressor. *Cell* **149**, 146–158 (2012).
541 53. Montgomery, R. K. *et al.* Mouse telomerase reverse transcriptase (mTert)
542 expression marks slowly cycling intestinal stem cells. *Proc. Natl. Acad. Sci. U. S.*
543 *A.* **108**, 179–184 (2011).
544 54. Muñoz, J. *et al.* The Lgr5 intestinal stem cell signature: robust expression of
545 proposed quiescent '+4' cell markers. *EMBO J.* **31**, 3079–3091 (2012).
546 55. Zhang, F. *et al.* Clusterin facilitates stress-induced lipidation of LC3 and
547 autophagosome biogenesis to enhance cancer cell survival. *Nat. Commun.* **5**,
548 5775 (2014).

549 56. Koltai, T. Clusterin: a key player in cancer chemoresistance and its inhibition.
550 *Onco. Targets. Ther.* **7**, 447–456 (2014).
551 57. Oliveira, C. S. F. *et al.* Cathepsin D protects colorectal cancer cells from acetate-
552 induced apoptosis through autophagy-independent degradation of damaged
553 mitochondria. *Cell Death Dis.* **6**, e1788–e1788 (2015).
554 58. Mahajan, U. M. *et al.* Cathepsin D Expression and Gemcitabine Resistance in
555 Pancreatic Cancer. *JNCI Cancer Spectr.* **4**, (2020).
556 59. Liu, R., Wettersten, H. I., Park, S.-H. & Weiss, R. H. Small-molecule inhibitors of
557 p21 as novel therapeutics for chemotherapy-resistant kidney cancer. *Future Med.*
558 *Chem.* **5**, 991–994 (2013).
559 60. Xia, X. *et al.* Cytoplasmic p21 is a potential predictor for cisplatin sensitivity in
560 ovarian cancer. *BMC Cancer* **11**, 399 (2011).
561 61. Koster, R. *et al.* Cytoplasmic p21 expression levels determine cisplatin resistance
562 in human testicular cancer. *J. Clin. Invest.* **120**, 3594–3605 (2010).
563 62. Maiuthed, A. *et al.* Cytoplasmic p21 Mediates 5-Fluorouracil Resistance by
564 Inhibiting Pro-Apoptotic Chk2. *Cancers (Basel).* **10**, 373 (2018).
565 63. Morris-Hanon, O. *et al.* The Cell Cycle Inhibitors p21(Cip1) and p27(Kip1) Control
566 Proliferation but Enhance DNA Damage Resistance of Glioma Stem Cells.
567 *Neoplasia* **19**, 519–529 (2017).
568 64. Jain, A. *et al.* Epithelial membrane protein-1 is a biomarker of gefitinib resistance.
569 *Proc. Natl. Acad. Sci. U. S. A.* **102**, 11858 LP – 11863 (2005).
570 65. Ariës, I. M. *et al.* EMP1, a novel poor prognostic factor in pediatric leukemia
571 regulates prednisolone resistance, cell proliferation, migration and adhesion.

Leukemia **28**, 1828–1837 (2014).

66. Lesuffleur, T. *et al.* Differential expression of the human mucin genes MUC1 to MUC5 in relation to growth and differentiation of different mucus-secreting HT-29 cell subpopulations. *J. Cell Sci.* **106**, 771 LP – 783 (1993).

67. Huang, D., Du, C., Ji, D., Xi, J. & Gu, J. Overexpression of LAMC2 predicts poor prognosis in colorectal cancer patients and promotes cancer cell proliferation, migration, and invasion. *Tumor Biol.* **39**, 1010428317705849 (2017).

68. Asfaha, S. *et al.* Krt19(+)/Lgr5(-) Cells Are Radioresistant Cancer-Initiating Stem Cells in the Colon and Intestine. *Cell Stem Cell* **16**, 627–638 (2015).

69. Wang, H. *et al.* LGALS3 Promotes Treatment Resistance in Glioblastoma and Is Associated with Tumor Risk and Prognosis. *Cancer Epidemiol. Biomarkers & Prev.* **28**, 760 LP – 769 (2019).

70. Stewart, R. L. & O'Connor, K. L. Clinical significance of the integrin α6β4 in human malignancies. *Lab. Invest.* **95**, 976–986 (2015).

71. Folgiero, V. *et al.* Induction of ErbB-3 Expression by α6β4 Integrin Contributes to Tamoxifen Resistance in ERβ1-Negative Breast Carcinomas. *PLoS One* **3**, e1592 (2008).

72. Qiu, H. *et al.* Targeting CDH17 suppresses tumor progression in gastric cancer by downregulating Wnt/β-catenin signaling. *PLoS One* **8**, e56959–e56959 (2013).

73. Atukorala, I. & Mathivanan, S. PO-066 Knockdown of cadherin 17 inactivates WNT signalling pathway and induces apoptosis in colorectal cancer cells. *ESMO Open* **3**, A47 (2018).

74. Ilmer, M. *et al.* Cell surface galectin-3 defines a subset of chemoresistant

595 gastrointestinal tumor-initiating cancer cells with heightened stem cell
596 characteristics. *Cell Death Dis.* **7**, e2337–e2337 (2016).
597 75. Chung, L.-Y. *et al.* Galectin-3 augments tumor initiating property and
598 tumorigenicity of lung cancer through interaction with β-catenin. *Oncotarget* **6**,
599 4936–4952 (2015).
600 76. Itahana, K. *et al.* A Role for p53 in Maintaining and Establishing the Quiescence
601 Growth Arrest in Human Cells. *J. Biol. Chem.* **277**, 18206–18214 (2002).
602 77. Meletis, K. *et al.* p53 suppresses the self-renewal of adult neural stem cells.
603 *Development* **133**, 363 LP – 369 (2006).
604 78. Liu, Y. *et al.* p53 regulates hematopoietic stem cell quiescence. *Cell Stem Cell* **4**,
605 37–48 (2009).
606 79. Lane, D. P. p53, guardian of the genome. *Nature* **358**, 15–16 (1992).
607 80. Liu, W., Guan, M., Hu, T., Gu, X. & Lu, Y. Re-Expression of AKAP12 Inhibits
608 Progression and Metastasis Potential of Colorectal Carcinoma In Vivo and In
609 Vitro. *PLoS One* **6**, e24015 (2011).
610 81. Lin, X., Nelson, P. & Gelman, I. H. SSeCKS, a major protein kinase C substrate
611 with tumor suppressor activity, regulates G(1)-->S progression by controlling the
612 expression and cellular compartmentalization of cyclin D. *Mol. Cell. Biol.* **20**,
613 7259–7272 (2000).
614 82. Gelman, I. H. Emerging Roles for SSeCKS/Gravin/AKAP12 in the Control of Cell
615 Proliferation, Cancer Malignancy, and Barriergenesis. *Genes Cancer* **1**, 1147–
616 1156 (2010).
617 83. Reggi, E. & Diviani, D. The role of A-kinase anchoring proteins in cancer

development. *Cell. Signal.* **40**, 143–155 (2017).

84. Hur, J. *et al.* CD82/KAI1 Maintains the Dormancy of Long-Term Hematopoietic Stem Cells through Interaction with DARC-Expressing Macrophages. *Cell Stem Cell* **18**, 508–521 (2016).

85. Xiong, Y. *et al.* p21 is a universal inhibitor of cyclin kinases. *Nature* **366**, 701–704 (1993).

86. El-Deiry, W. WAF1, a potential mediator of p53 tumor suppression. *Cell* **75**, 817–825 (1993).

87. Vogelstein, B., Lane, D. & Levine, A. J. Surfing the p53 network. *Nature* **408**, 307–310 (2000).

88. Wade Harper, J. The p21 Cdk-interacting protein Cip1 is a potent inhibitor of G1 cyclin-dependent kinases. *Cell* **75**, 805–816 (1993).

89. Labalette, C. *et al.* The LIM-only protein FHL2 regulates cyclin D1 expression and cell proliferation. *J. Biol. Chem.* **283**, 15201–15208 (2008).

90. Martin, B. T. *et al.* FHL2 Regulates Cell Cycle-Dependent and Doxorubicin-Induced p21Cip1/Waf1 Expression in Breast Cancer Cells. *Cell Cycle* **6**, 1779–1788 (2007).

91. Hellerbrand. FHL2 suppresses growth and differentiation of the colon cancer cell line HT-29. *Oncol. Rep.* **23**, (2010).

92. Lee, S.-W., Kim, E.-J. & Um, S.-J. FHL2 mediates p53-induced transcriptional activation through a direct association with HIPK2. *Biochem. Biophys. Res. Commun.* **339**, 1056–1062 (2006).

93. An, B. C. *et al.* GPx3-mediated redox signaling arrests the cell cycle and acts as a

641 tumor suppressor in lung cancer cell lines. *PLoS One* **13**, e0204170–e0204170
642 (2018).
643 94. Barrett, C. W. *et al.* Tumor suppressor function of the plasma glutathione
644 peroxidase gpx3 in colitis-associated carcinoma. *Cancer Res.* **73**, 1245–1255
645 (2013).
646 95. Wang, H. *et al.* p53-induced gene 3 mediates cell death induced by glutathione
647 peroxidase 3. *J. Biol. Chem.* **287**, 16890–16902 (2012).
648 96. Polato, F. *et al.* DRAGO (KIAA0247), a new DNA damage-responsive, p53-
649 inducible gene that cooperates with p53 as oncosuppressor. [Corrected]. *J. Natl.*
650 *Cancer Inst.* **106**, dju053–dju053 (2014).
651 97. Huang, C.-J. *et al.* A predicted protein, KIAA0247, is a cell cycle modulator in
652 colorectal cancer cells under 5-FU treatment. *J. Transl. Med.* **9**, 82 (2011).
653 98. Kim, S.-L. *et al.* Lipocalin 2 negatively regulates cell proliferation and epithelial to
654 mesenchymal transition through changing metabolic gene expression in colorectal
655 cancer. *Cancer Sci.* **108**, 2176–2186 (2017).
656 99. Chakraborty, S., Kaur, S., Guha, S. & Batra, S. K. The multifaceted roles of
657 neutrophil gelatinase associated lipocalin (NGAL) in inflammation and cancer.
658 *Biochim. Biophys. Acta - Rev. Cancer* **1826**, 129–169 (2012).
659 100. Chiang, K.-C. *et al.* Lipocalin 2 (LCN2) is a promising target for
660 cholangiocarcinoma treatment and bile LCN2 level is a potential
661 cholangiocarcinoma diagnostic marker. *Sci. Rep.* **6**, 36138 (2016).
662 101. Tu, S. P. *et al.* p53 inhibition of AP1-dependent TFF2 expression induces
663 apoptosis and inhibits cell migration in gastric cancer cells. *Am. J. Physiol. Liver*

Physiol. **297**, G385–G396 (2009).

102. Dubeykovskaya, Z. *et al.* Neural innervation stimulates splenic TFF2 to arrest myeloid cell expansion and cancer. *Nat. Commun.* **7**, 10517 (2016).

103. Dubeykovskaya, Z. A. *et al.* Therapeutic potential of adenovirus-mediated TFF2-CTP-Flag peptide for treatment of colorectal cancer. *Cancer Gene Ther.* **26**, 48–57 (2019).

104. Thim, L. Trefoil peptides: from structure to function. *Cell. Mol. Life Sci. C.* **53**, 888–903 (1997).

105. Bossenmeyer-Pourié, C. *et al.* The trefoil factor 1 participates in gastrointestinal cell differentiation by delaying G1-S phase transition and reducing apoptosis . *J. Cell Biol.* **157**, 761–770 (2002).

106. Huang, Y., Zhu, Y., Zhang, Z., Li, Z. & Kong, C. UNC5B mediates G2/M phase arrest of bladder cancer cells by binding to CDC14A and P53. *Cancer Gene Ther.* (2020). doi:10.1038/s41417-020-0175-x

107. Okazaki, S. Clinical significance of UNC5B expression in colorectal cancer. *Int. J. Oncol.* (2011). doi:10.3892/ijo.2011.1201

108. Kong, C. *et al.* Overexpression of UNC5B in bladder cancer cells inhibits proliferation and reduces the volume of transplantation tumors in nude mice. *BMC Cancer* **16**, 892 (2016).

109. Bersani, C., Xu, L.-D., Vilborg, A., Lui, W.-O. & Wiman, K. G. Wig-1 regulates cell cycle arrest and cell death through the p53 targets FAS and 14-3-3σ. *Oncogene* **33**, 4407–4417 (2014).

110. Hellborg, F. *et al.* Human wig-1, a p53 target gene that encodes a growth

687 inhibitory zinc finger protein. *Oncogene* **20**, 5466–5474 (2001).
688 111. Rouillard, A. D. *et al.* The harmonizome: a collection of processed datasets
689 gathered to serve and mine knowledge about genes and proteins. *Database*
690 **2016**, (2016).
691 112. Marreiros, A. *et al.* KAI1 promoter activity is dependent on p53, junB and AP2:
692 evidence for a possible mechanism underlying loss of KAI1 expression in cancer
693 cells. *Oncogene* **24**, 637–649 (2005).
694 113. Soutto, M. *et al.* TFF1 activates p53 through down-regulation of miR-504 in
695 gastric cancer. *Oncotarget* **5**, 5663–5673 (2014).
696 114. Fischer, M. Census and evaluation of p53 target genes. *Oncogene* **36**, 3943–
697 3956 (2017).
698 115. Miyamoto, T. *et al.* Lipocalin 2 Enhances Migration and Resistance against
699 Cisplatin in Endometrial Carcinoma Cells. *PLoS One* **11**, e0155220–e0155220
700 (2016).
701 116. Alexander, M. S. *et al.* CD82 Is a Marker for Prospective Isolation of Human
702 Muscle Satellite Cells and Is Linked to Muscular Dystrophies. *Cell Stem Cell* **19**,
703 800–807 (2016).
704 117. Georgakilas, A. G., Martin, O. A. & Bonner, W. M. p21: A Two-Faced Genome
705 Guardian. *Trends Mol. Med.* **23**, 310–319 (2017).
706 118. Cheng, T. Hematopoietic Stem Cell Quiescence Maintained by p21cip1/waf1.
707 *Science (80-.).* **287**, 1804–1808 (2000).
708 119. Kippin, T. E., Martens, D. J. & van der Kooy, D. p21 loss compromises the relative
709 quiescence of forebrain stem cell proliferation leading to exhaustion of their

710 proliferation capacity. *Genes Dev.* **19**, 756–767 (2005).
711 120. Smith, G. H. Label-retaining epithelial cells in mouse mammary gland divide
712 asymmetrically and retain their template DNA strands. *Development* **132**, 681–
713 687 (2005).
714 121. Wilson, A. *et al.* Hematopoietic stem cells reversibly switch from dormancy to self-
715 renewal during homeostasis and repair. *Cell* **135**, 1118–29 (2008).
716 122. Cotsarelis, G., Sun, T.-T. & Lavker, R. M. Label-retaining cells reside in the bulge
717 area of pilosebaceous unit: Implications for follicular stem cells, hair cycle, and
718 skin carcinogenesis. *Cell* **61**, 1329–1337 (1990).
719 123. RUBIO, C. A. Arrest of Cell Proliferation in Budding Tumor Cells Ahead of the
720 Invading Edge of Colonic Carcinomas. A Preliminary Report. *Anticancer Res.* **28**,
721 2417–2420 (2008).
722 124. Harbaum, L. *et al.* Keratin 7 expression in colorectal cancer – freak of nature or
723 significant finding? *Histopathology* **59**, 225–234 (2011).
724 125. De Smedt, L. *et al.* Expression profiling of budding cells in colorectal cancer
725 reveals an EMT-like phenotype and molecular subtype switching. *Br. J. Cancer*
726 **116**, 58–65 (2017).
727 126. Jung, A. *et al.* The Invasion Front of Human Colorectal Adenocarcinomas Shows
728 Co-Localization of Nuclear β-Catenin, Cyclin D_1, and $p16^{INK4A}$ and Is a
729 Region of Low Proliferation. *Am. J. Pathol.* **159**, 1613–1617 (2001).
730 127. Dawson, H. *et al.* The apoptotic and proliferation rate of tumour budding cells in
731 colorectal cancer outlines a heterogeneous population of cells with various
732 impacts on clinical outcome. *Histopathology* **64**, 577–584 (2014).

128. Cho, I. J. *et al.* Mechanisms, Hallmarks, and Implications of Stem Cell Quiescence. *Stem cell reports* **12**, 1190–1200 (2019).

129. Schepeler, T., Mansilla, F., Christensen, L. L., Orntoft, T. F. & Andersen, C. L. Clusterin expression can be modulated by changes in TCF1-mediated Wnt signaling. *J. Mol. Signal.* **2**, 6 (2007).

130. Basu, S. *et al.* Increased expression of cathepsin D is required for L1-mediated colon cancer progression. *Oncotarget* **10**, 5217–5228 (2019).

131. Xu, J. *et al.* β-catenin regulates c-Myc and CDKN1A expression in breast cancer cells. *Mol. Carcinog.* **55**, 431–439 (2016).

132. Yao, H. *et al.* AV-65, a novel Wnt/β-catenin signal inhibitor, successfully suppresses progression of multiple myeloma in a mouse model. *Blood Cancer J.* **1**, e43–e43 (2011).

133. Pai, P., Rachagani, S., Dhawan, P. & Batra, S. K. Mucins and Wnt/β-catenin signaling in gastrointestinal cancers: an unholy nexus. *Carcinogenesis* **37**, 223–232 (2016).

134. Sánchez-Tilló, E. *et al.* β-catenin/TCF4 complex induces the epithelial-to-mesenchymal transition (EMT)-activator ZEB1 to regulate tumor invasiveness. *Proc. Natl. Acad. Sci.* **108**, 19204 LP – 19209 (2011).

135. Saha, S. K. *et al.* KRT19 directly interacts with β-catenin/RAC1 complex to regulate NUMB-dependent NOTCH signaling pathway and breast cancer properties. *Oncogene* **36**, 332–349 (2017).

136. Korkmaz, G. *et al.* LGALS3 and AXIN1 gene variants playing role in the Wnt/ β-catenin signaling pathway are associated with mucinous component and tumor

size in colorectal cancer. *Bosn. J. basic Med. Sci.* **16**, 108–113 (2016).

137. Kinchen, J. *et al.* Structural Remodeling of the Human Colonic Mesenchyme in Inflammatory Bowel Disease. *Cell* **175**, 372-386.e17 (2018).

138. Camps, J. *et al.* Interstitial Cell Remodeling Promotes Aberrant Adipogenesis in Dystrophic Muscles. *Cell Rep.* **31**, (2020).

139. Avvisato, C. L. *et al.* Mechanical force modulates global gene expression and β-catenin signaling in colon cancer cells. *J. Cell Sci.* **120**, 2672 LP – 2682 (2007).

140. Wang, Y. *et al.* Anti-Cadherin-17 Antibody Modulates Beta-Catenin Signaling and Tumorigenicity of Hepatocellular Carcinoma. *PLoS One* **8**, e72386 (2013).

141. Shimura, T. *et al.* Galectin-3, a Novel Binding Partner of β-Catenin. *Cancer Res.* **64**, 6363 LP – 6367 (2004).

142. Regan, J. L. Cell fate in colon cancer stem cells: To GLI or not to GLI? *Mol. Cell. Oncol.* **5**, e1445940–e1445940 (2018).

143. Vousden, K. H. & Lane, D. P. p53 in health and disease. *Nat. Rev. Mol. Cell Biol.* **8**, 275–283 (2007).

144. Jain, A. K. & Barton, M. C. p53: emerging roles in stem cells, development and beyond. *Development* **145**, dev158360 (2018).

145. Tosoni, D. *et al.* The Numb/p53 circuitry couples replicative self-renewal and tumor suppression in mammary epithelial cells. *J. Cell Biol.* **211**, 845–862 (2015).

146. Zhao, Z. *et al.* p53 loss promotes acute myeloid leukemia by enabling aberrant self-renewal. *Genes Dev.* **24**, 1389–1402 (2010).

147. Tschaharganeh, D. F. *et al.* p53-Dependent Nestin Regulation Links Tumor Suppression to Cellular Plasticity in Liver Cancer. *Cell* **158**, 579–592 (2014).

148. Freed-Pastor, W. A. *et al.* Mutant p53 disrupts mammary tissue architecture via the mevalonate pathway. *Cell* **148**, 244–258 (2012).

149. McConnell, A. M. *et al.* p53 Regulates Progenitor Cell Quiescence and Differentiation in the Airway. *Cell Rep.* **17**, 2173–2182 (2016).

150. Zheng, H. *et al.* p53 and Pten control neural and glioma stem/progenitor cell renewal and differentiation. *Nature* **455**, 1129–1133 (2008).

151. Flamini, V. *et al.* The Satellite Cell Niche Regulates the Balance between Myoblast Differentiation and Self-Renewal via p53. *Stem cell reports* **10**, 970–983 (2018).

152. Deng, C., Zhang, P., Wade Harper, J., Elledge, S. J. & Leder, P. Mice Lacking p21CIP1/WAF1 undergo normal development, but are defective in G1 checkpoint control. *Cell* **82**, 675–684 (1995).

153. Brugarolas, J. *et al.* Radiation-induced cell cycle arrest compromised by p21 deficiency. *Nature* **377**, 552–557 (1995).

154. Kobayashi, A. *et al.* Bone morphogenetic protein 7 in dormancy and metastasis of prostate cancer stem-like cells in bone. *J. Exp. Med.* **208**, 2641–2655 (2011).

155. Takeishi, S. *et al.* Ablation of Fbxw7 Eliminates Leukemia-Initiating Cells by Preventing Quiescence. *Cancer Cell* **23**, 347–361 (2013).

156. Levine, A. J. Targeting Therapies for the p53 Protein in Cancer Treatments. *Annu. Rev. Cancer Biol.* **3**, 21–34 (2019).

157. Jackson, J. G. *et al.* p53-Mediated Senescence Impairs the Apoptotic Response to Chemotherapy and Clinical Outcome in Breast Cancer. *Cancer Cell* **21**, 793–806 (2012).

158. Ungerleider, N. A. *et al.* Breast cancer survival predicted by TP53 mutation status differs markedly depending on treatment. *Breast Cancer Res.* **20**, 115 (2018).

159. Rogel, A., Popliker, M., Webb, C. G. & Oren, M. p53 cellular tumor antigen: analysis of mRNA levels in normal adult tissues, embryos, and tumors. *Mol. Cell. Biol.* **5**, 2851 LP – 2855 (1985).

160. Webster, M. R. *et al.* Paradoxical Role for Wild-Type p53 in Driving Therapy Resistance in Melanoma. *Mol. Cell* **77**, 633-644.e5 (2020).

161. Choudhury, A. R. *et al.* Cdkn1a deletion improves stem cell function and lifespan of mice with dysfunctional telomeres without accelerating cancer formation. *Nat. Genet.* **39**, 99–105 (2007).

162. El-Deiry, W. S. p21(WAF1) Mediates Cell-Cycle Inhibition, Relevant to Cancer Suppression and Therapy. *Cancer Res.* **76**, 5189–5191 (2016).

163. Weiss, R. H. $p21^{Waf1/Cip1}$ as a therapeutic target in breast and other cancers. *Cancer Cell* **4**, 425–429 (2003).

164. Viale, A. *et al.* Cell-cycle restriction limits DNA damage and maintains self-renewal of leukaemia stem cells. *Nature* **457**, 51–56 (2009).

165. Hui Tian, E. K. W. and T. J. J. p21WAF1/CIP1 Antisense Therapy Radiosensitizes Human Colon Cancer by Converting Growth Arrest to Apoptosis. *Cancer Res* **60**, 679–684 (2000).

166. Kokunai, T., Urui, S., Tomita, H. & Tamaki, N. Overcoming of Radioresistance in Human Gliomas by p21WAF1/CIP1 Antisense Oligonucleotide. *J. Neurooncol.* **51**, 111–119 (2001).

167. Joanna K Sax, Bipin C Dash, Rui Hong, David T Dicker, W. S. E.-D. The Cyclin-

Dependent Kinase Inhibitor Butyrolactone Is a Potent Inhibitor of p21 WAF1/CIP1 Expression. *Cell Cycle* **1**, 87–93 (2002).

168. Park, S.-H., Wang, X., Liu, R., Lam, K. S. & Weiss, R. H. High throughput screening of a small molecule one-bead-one-compound combinatorial library to identify attenuators of p21 as chemotherapy sensitizers. *Cancer Biol. Ther.* **7**, 2015–2022 (2008).

169. Inoue, H., Hwang, S. H., Wecksler, A. T., Hammock, B. D. & Weiss, R. H. Sorafenib attenuates p21 in kidney cancer cells and augments cell death in combination with DNA-damaging chemotherapy. *Cancer Biol. Ther.* **12**, 827–836 (2011).

170. Wettersten, H. I. *et al.* A novel p21 attenuator which is structurally related to sorafenib. *Cancer Biol. Ther.* **14**, 278–285 (2013).

171. Sato, T. *et al.* Long-term Expansion of Epithelial Organoids From Human Colon, Adenoma, Adenocarcinoma, and Barrett's Epithelium. *Gastroenterology* **141**, 1762–1772 (2011).

172. Love, M. I., Huber, W. & Anders, S. Moderated estimation of fold change and dispersion for RNA-seq data with DESeq2. *Genome Biol.* **15**, 550 (2014).

173. Nagy, Á., Lánczky, A., Menyhárt, O. & Győrffy, B. Validation of miRNA prognostic power in hepatocellular carcinoma using expression data of independent datasets. *Sci. Rep.* **8**, 9227 (2018).

174. Ashburner, M. *et al.* Gene Ontology: tool for the unification of biology. *Nat. Genet.* **25**, 25–29 (2000).

175. The Gene Ontology Consortium. The Gene Ontology Resource: 20 years and still

GOing strong. *Nucleic Acids Res.* **47**, D330–D338 (2018).

176. Cumming, G., Fidler, F. & Vaux, D. L. Error bars in experimental biology. *J Cell Biol* **177**, 7–11 (2007).

177. Subramanian, A. *et al.* Gene set enrichment analysis: a knowledge-based approach for interpreting genome-wide expression profiles. *Proc. Natl. Acad. Sci. U. S. A.* **102**, 15545–15550 (2005).

178. Liberzon, A. *et al.* The Molecular Signatures Database Hallmark Gene Set Collection. *Cell Syst.* **1**, 417–425 (2015).

179. Benjamini, Y. & Hochberg, Y. Controlling the false discovery rate: a practical and powerful approach to multiple testing. *J R Stat. Soc B* **57**, 289–300 (1995).

FIGURE LEGENDS

Figure 1. Colon cancer PDOs contain a subpopulation of non-cycling cells

(A) Phase contrast image of colon cancer PDOs labelled with cell-tracker dye CM-DiL after 72 h (Bar = 75 µm) (see also Table S1). (B) Representative FACS plots of EdU cell cycle analysis of 151-ML-M PDO cells at 2 h (left hand side) and 72 h (right hand side) after labelling. (C) Percentage of cells (±SD) in G0/1, G2/M and S Phase at 2 h and 72 h post EdU labelling in PDO models 151-ML-M, 162-MW-P, 195-CB-P, 249-CB-P, 278-ML-P and 302-CB-M (data from three independent experiments).

Figure 2. Non-cycling PDO cells are quiescent CSCs that can re-enter cell cycle and persist long-term *in vivo*

(A) Representative FACS plot of PKH26 labelled 278-ML-P PDO cells after 12 h (middle panel) and 12 days (right side panel) compared to non-labelled control (left side panel). (B) Frequency (±SD) of $PKH26^{Positive}$ LRCs in PDO models after 12 days (data from 5 independent experiments). (C) FACS histograms demonstrating frequency of $PKH26^{Positive}$ cells in 151-ML-M PDOs at 12 h (left side panel) and 12 days (middle panel) after staining and 24 days (right side panel) after FACS isolation and serial replating of $PKH26^{Positive}$ cells from 12 day cultures. (D) Phase contrast of unlabeled PDOs (negative control) (Bar = 100 μm) and (E) immunofluorescence images of PKH26 labelled PDOs at 12 h and 12 days (left and middle panels) and 24 days after FACS isolation and serial re-plating of $PKH26^{Positive}$ LRCs from 12 day cultures (right side panel). Cells are stained for F-ACTIN (green) and nuclei are counterstained with DAPI (blue) (Bars = 20 μm). (F) Mean colony size (±SD) of $PKH26^{Negative}$ and $PKH26^{Positive}$ cell derived PDOs in Matrigel culture. Data from three independent experiments. **p-value: < 0.01 (t test). (G) Limiting dilution spheroid formation assay of $PKH26^{Negative}$ and $PKH26^{Positive}$ cells. Data from three independent experiments. The p-values for pairwise tests of differences in CSC frequencies between $PKH26^{Negative}$ and $PKH26^{Positive}$ cells in 151-ML-M, 162-MW-P, 195-CB-P, 249-CB-P, 278-ML-P and 302-CB-M tumors are 1.27×10^{-13}, 1.87×10^{-5}, 6.42×10^{-11}, 1.12×10^{-10}, 3.5×10^{-14}, 6.14×10^{-12}, respectively. (H) Immunofluorescence image of a frozen PDX section derived from 1,000 PKH26 labelled 195-CB-P PDO cells 80 days post transplantation. Magnified region indicates a long-term label-retaining $PKH26^{Positive}$ cell. Cells are stained for α-tubulin (green) and nuclei are counterstained with DAPI (blue) (Bar = 100μm).

Figure 3. PKH26^{Positive} qCSCs are enriched for stem cell associated gene sets and p53-interacting negative regulators of proliferation and have downregulated expression of cell cycle genes

(A) RNA sequencing generated gene set enrichment analysis for organ development (nominal p-value = < 0.0005), cell development (nominal p-value = < 0.0005), nervous system development (nominal p-value = < 0.0005), embryonic development (nominal p-value = 0.03), placenta (nominal p-value = < 0.0005), epithelial mesenchymal transition (nominal p-value = < 0.0005), p53 pathway (nominal p-value = < 0.0005), TNFa signaling via NFkB (nominal p-value = < 0.0005), Wnt signaling pathway (nominal p-value = 0.002) and hedgehog signaling pathway (nominal p-value = 0.002) in 12 day PKH26^{Positive} LRCs (compared to PKH26^{Negative} cells) from PDO models 151-ML-M, 162-MW-P, 195-CB-P, 249-CB-P, 278-ML-P and 302-CB-M (n = 4 separate cell preparations). (B) Gene ontology (GO) groups downregulated in PKH26^{Positive} LRCs. (C) Cell Cycle, transcription and protein synthesis GO terms downregulated in PKH26^{Positive} LRCs. (D) RNA sequencing generated normalized counts for negative cell cycle regulator and p53 target genes *AKAP12, CD82, CDKN1A, FHL2, GPX3, KIAA0247, LCN2, TFF2, UNC5B* and *ZMAT3* in PKH26^{Negative} and PKH26^{Positive} cells. (E) Venn diagram shows the number of upregulated RNA-sequencing generated transcripts identified in intestinal revSCs (50 genes; log fold change > 0.25, p-value < 0.05) by Ayyaz *et al*. (2019)[15] and in PKH26^{Positive} qCSCs (255 genes; log2 fold change > 0.586, p-value < 0.05) and upregulated in both revSCs and PKH26^{Positive} qCSCs (14 genes; representation factor 21.8, p-value < 1.452e-15). The representation factor is the number of overlapping genes divided by the expected number of overlapping genes drawn from two independent groups. A representation factor > 1

indicates more overlap than expected of two independent groups. (F) Table shows the 14 genes upregulated in both revSCs and PKH26^{Positive} qCSCs. *ITM2C is a paralog of revSC enriched Itm2b. (See also Figure S1).

Figure 4. p53 target genes are indicators of poor prognosis and required for the maintenance of PKH26^{Positive} quiescent CSCs

(A) Kaplan-Meier survival curves for *AKAP12, CD82, CDKN1A, FHL2, GPX3, KIAA0247, LCN2, TFF2, UNC5B* and *ZMAT3* in colorectal cancer patients comparing lower quartile to upper quartile (logrank p-values = 2.2E-06, 0.004, 8.1E-05, 0.00012, 0.0003, 0.049, 0.00018, 5.7E-05 and 0.3, respectively). Of these, higher *AKAP12, CD82, CDKN1A, FHL2, GPX3, KIAA0247, LCN2, TFF2 and UNC5B* are significant at FDR < 10%. Results based upon data generated by the Kaplan-Meier Plotter (kmplot.com)[173]. (B) Representative FACS plot of PKH26 labelled 151-ML-M Control-GFP cells (top row) and shRNA CDKN1A-GFP cells (bottom row) after 12 h and 12 days. (C) Frequency (±SD) of PKH26^{Positive} LRCs in shRNA CDKN1A PDO models after 12 days compared to control virus transduced cells (data from 3 independent experiments). (See also Figure S2).

Figure 1

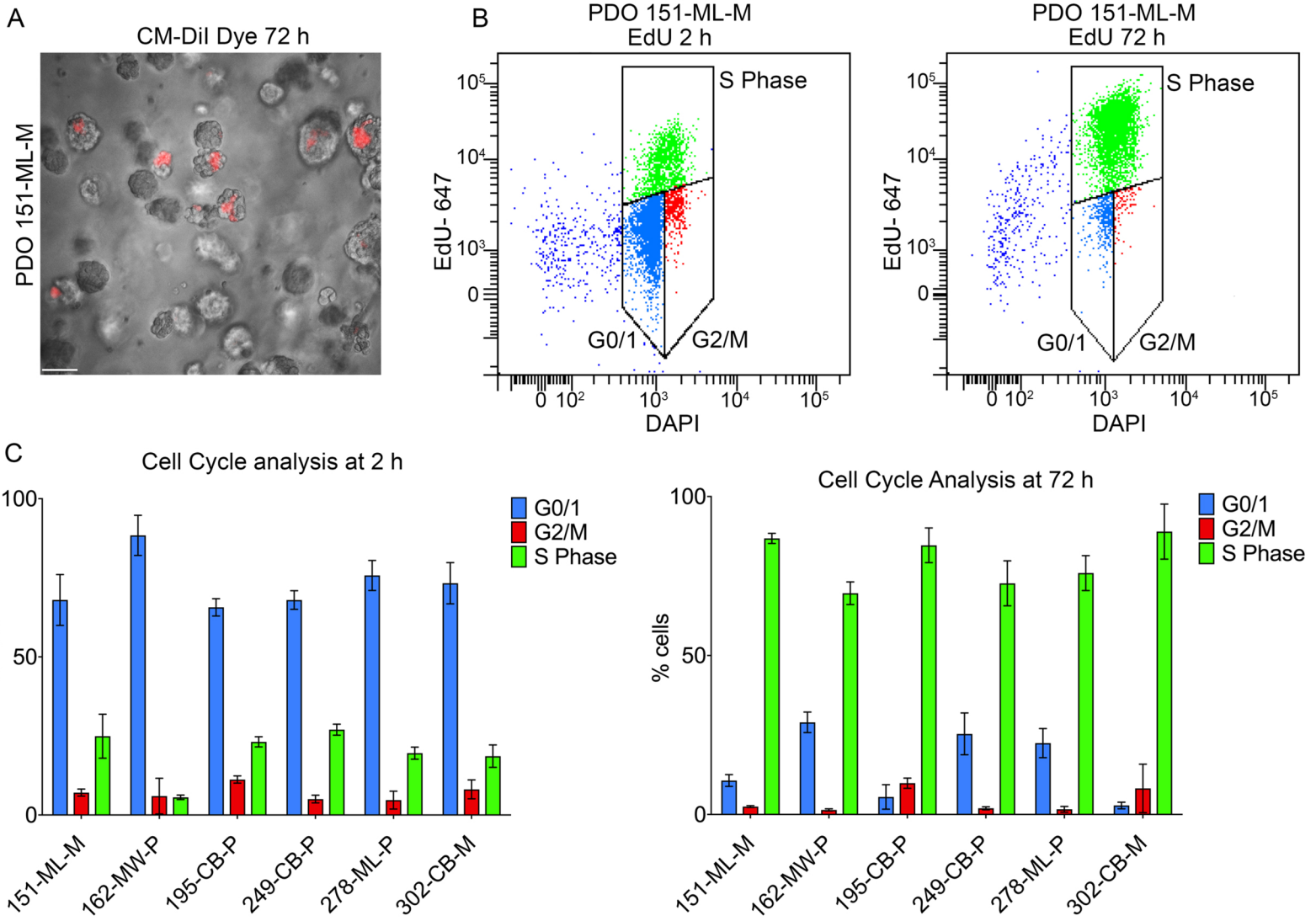

Figure 2

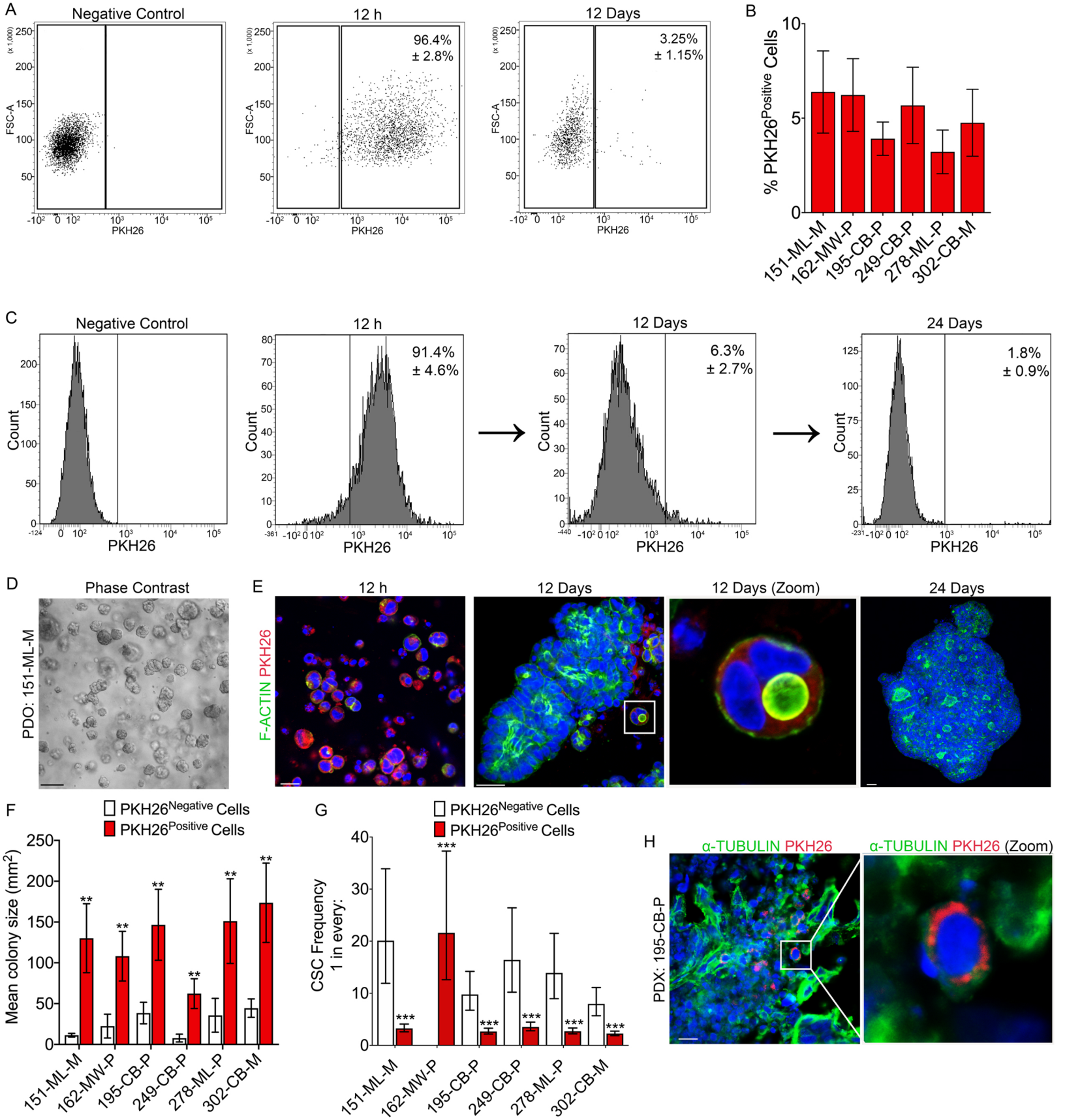

Figure 3

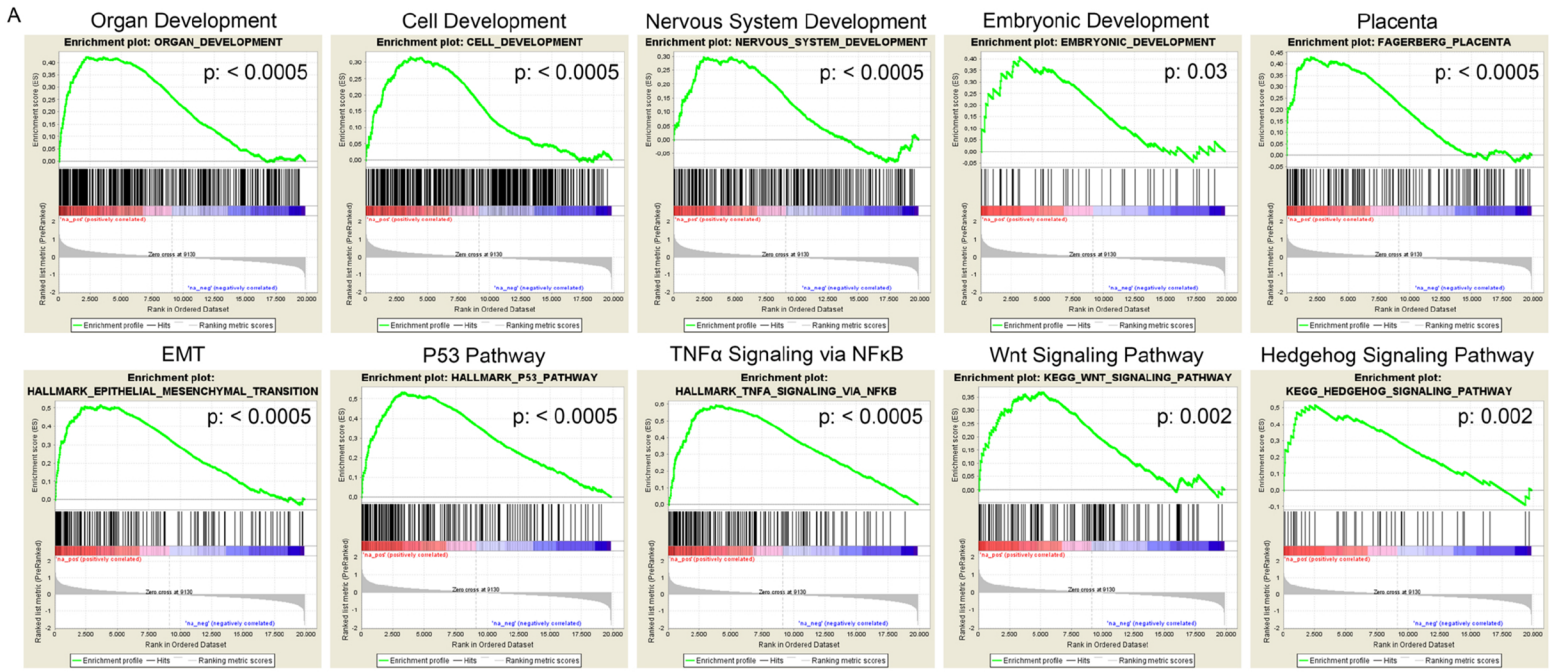

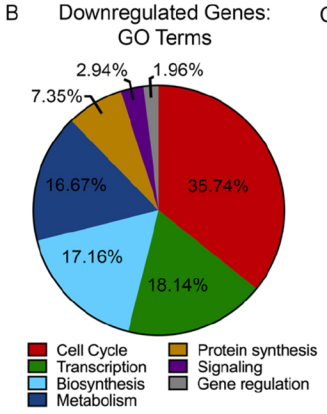

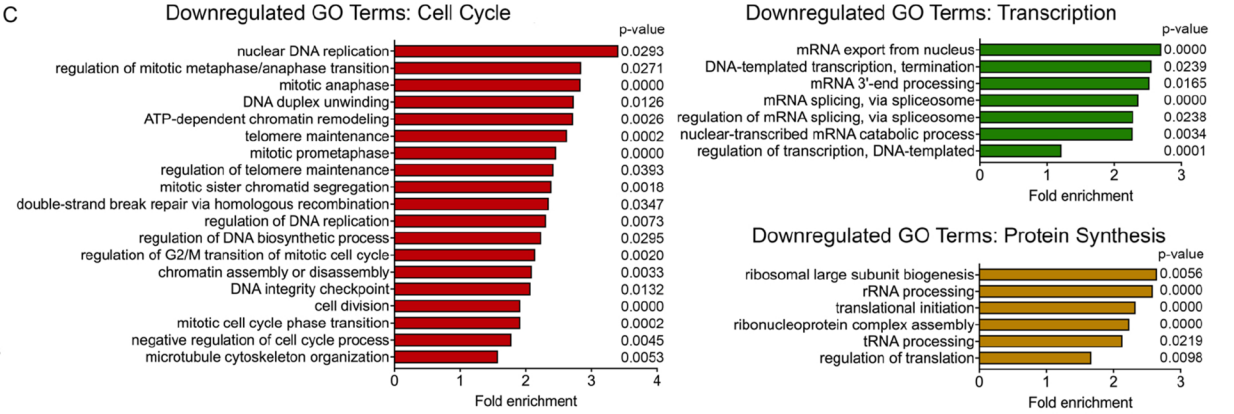

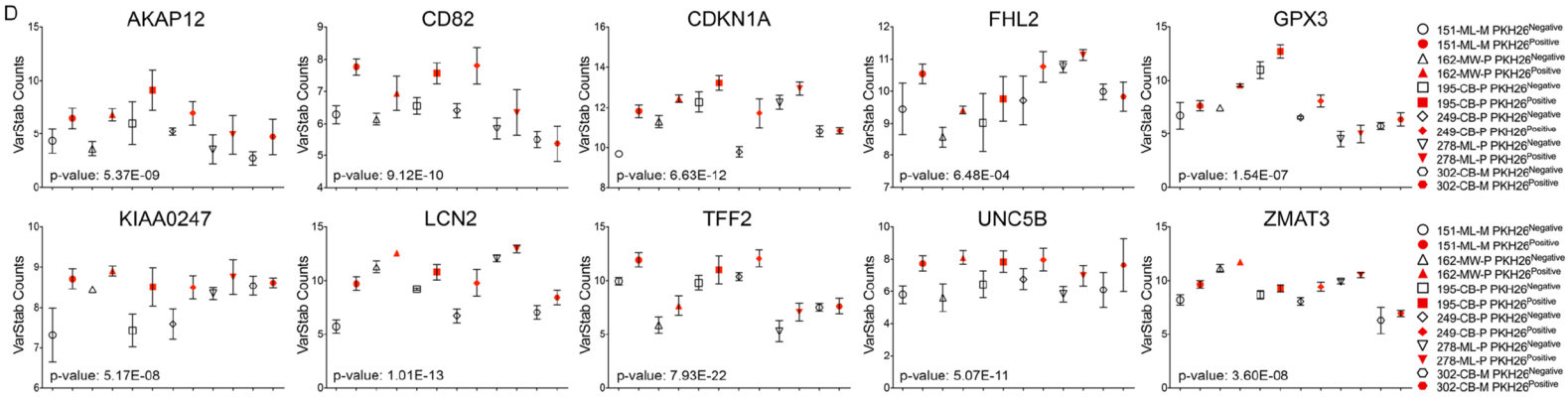

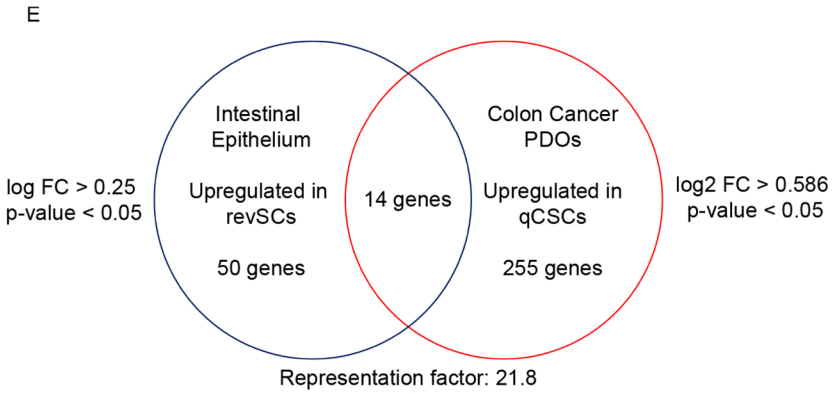

F

Gene Name	log2 Fold Change	p-value
CTSD	1.0362917	3.55E-12
CDKN1A	1.1134356	6.63E-12
GSN	0.93978	5.67E-10
ITGB4	0.74492633	2.08E-07
CDH17	0.9418327	3.78E-07
LGALS3	0.6010856	1.13E-06
KRT19	0.6341487	2.29E-05
MUC3A	0.7705268	3.13E-05
*ITM2C**	0.5946194	1.57E-04
AHNAK2	0.9683501	3.65E-04
CLU	0.9644593	1.03E-03
F3	0.8337223	1.27E-03
LAMC2	0.70564735	2.79E-03
EMP1	0.864138	1.06E-02

Figure 4

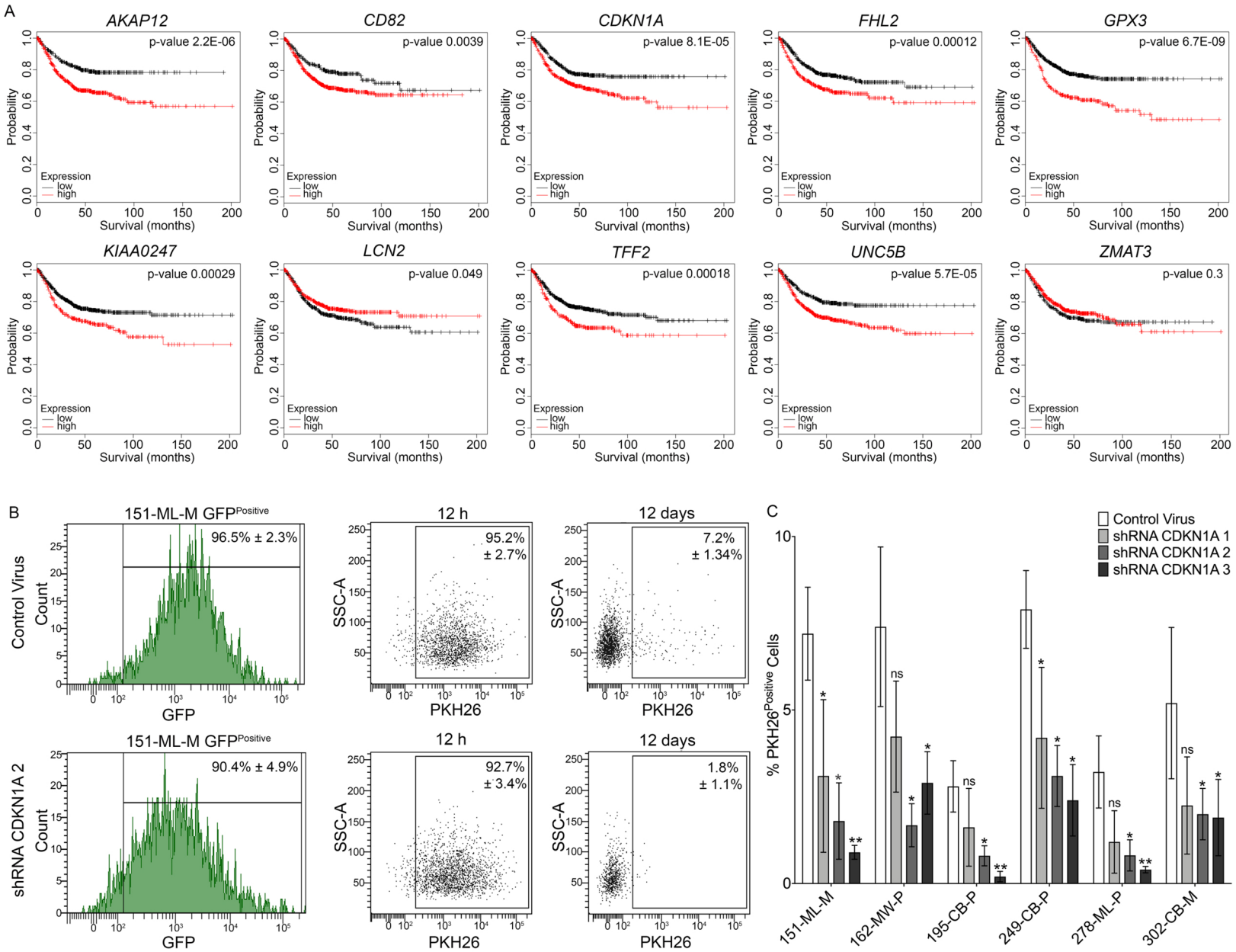

Supplemental Information

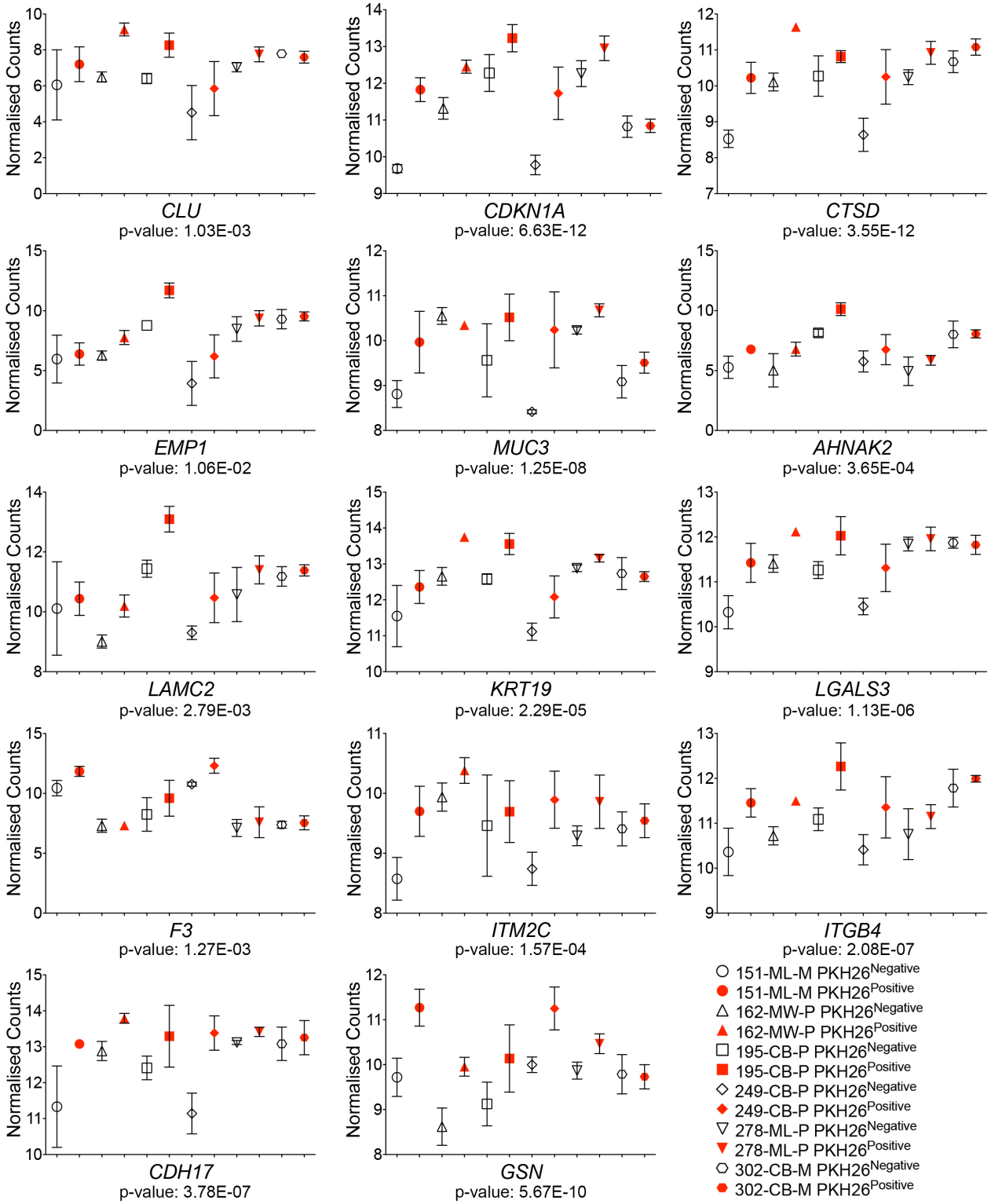

Figure S1: RNA-sequencing generated normalized counts for differentially expressed and common revSC[1] molecular signature genes in PKH26^{Positive} qCSCs compared to PKH26^{Negative} cells. Related to Figure 3.

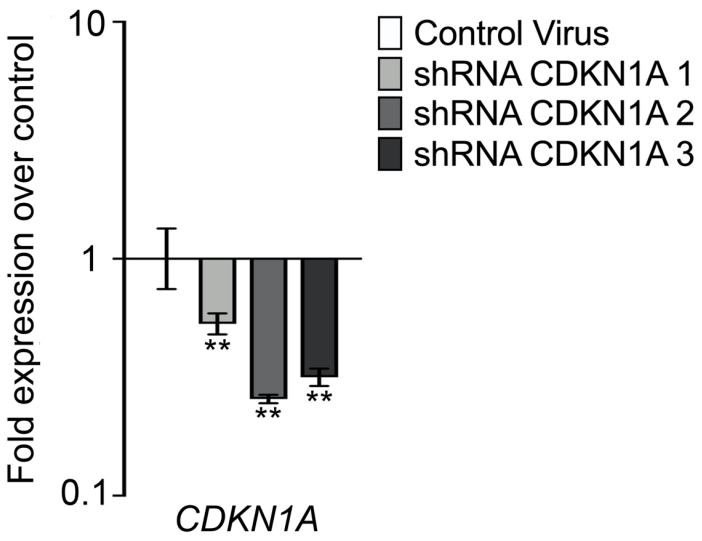

Figure S2: Fold expression of CDKN1A (±95% confidence intervals) in shRNA CDKN1A transduced PDOs from three independent experiments. Related to Figure 4.

Significant differences are *p-value < 0.05; **p-value < 0.01 and were determined by inspection of error bars as described by Cumming et al. (2007)[2].

Patient Model	Origin	TNM stage	Stage	P53 Status
151-ML-M	Liver	T2 N0 M0 , M1a	IVA	*SNV (G266E)
162-MW-P	Sigmoid colon & descending colon	T3 N0 M0	IIA	Wild type
195-CB-P	Sigmoid colon	T4a N2b M1a	IVA	*SNV (C135F)
249-CB-P	Ascending colon	T3 N0 M0	III	Wild type
278-ML-P	Sigmoid colon & descending colon	T4a N0 M0	IIB	*SNV (R273C)
302-CB-M	Liver	T3 N1a M1a	IVA	Wild type

Table S1 Tissue Origin, TNM Classification and P53 status of tumors. Related to Figure 1.

T: primary tumor size, N: regional lymph nodes involved, M: distant metastasis, *SNV: non-synonymous single nucleotide variant

LENTIVIRUS	SIGMA PRODUCT	PRODUCT NAME	VECTOR	TRC NUMBER
Control	SHC003V	MISSION® tGFP™ Positive Control Transduction Particles	–pLKO.1-puro-CMV-tGFP	NA
shCDKN1A 1	SHCLNV-NM_000389	CDKN1A MISSION shRNA Lentiviral Transduction Particles	–hPGK-Puro-CMV-tGFP	TRCN0000040123
shCDKN1A 2	SHCLNV-NM_000399	CDKN1A MISSION shRNA Lentiviral Transduction Particles	–hPGK-Puro-CMV-tGFP	TRCN0000287021
shCDKN1A 3	SHCLNV-NM_000399	CDKN1A MISSION shRNA Lentiviral Transduction Particles	–hPGK-Puro-CMV-tGFP	TRCN0000287091

Table S2. Lentiviral Transduction Particles. Related to Figure 4

Symbol	Gene Name	UniGene ID	TaqMan® Gene Expression Assay
CDKN1A	cyclin dependent kinase inhibitor 1A	Hs.370771	Hs00355782_m1
GAPDH	glyceraldehyde-3-phosphate dehydrogenase	Hs.544577	Hs02758991_g1

Table S3. Taqman® Gene Expression Assays. Related to Figure 4.

Supplementary Data 1

References

1. Ayyaz, A., Kumar, S., Sangiorgi, B., Ghoshal, B., Gosio, J., Ouladan, S., Fink, M., Barutcu, S., Trcka, D., Shen, J., Chan, K., Wrana, J. L. & Gregorieff, A. Single-cell transcriptomes of the regenerating intestine reveal a revival stem cell. Nature **569,** 121–125 (2019).
2. Cumming, G., Fidler, F. & Vaux, D. L. Error bars in experimental biology. J Cell Biol **177,** 7–11 (2007).